Decrease trend of East Asia dust during the 21st century in CMIP6

Wang Weijie[1] and Cheng Tiantao[2]

[1]Duke Kunshan University
[2]Fudan University

November 16, 2022

Abstract

A reduction of dust emission over the major dust source regions in East Asia in the twenty-first century is diagnosed in the climate change simulations of the Sixth Climate Model Intercomparison Project (CMIP6). Such change is attributable to the reduction of surface wind speeds in the dust source regions. To evaluate how the magnitude of warming affects dust emission, we examined two model scenarios, one high-forcing pathway and one medium-forcing pathway. We find dust optical depth over dust source regions would decrease by 5.6% by the end of the twenty-first century under the high-forcing pathway. Under the medium-forcing pathway, dust optical depth would decrease by less than 2%. These results provide a quantitative understanding of how global warming affects dust emission in the major dust source regions in East Asia.

Decrease trend of East Asia dust during the 21st century in CMIP6

Weijie Wang[1] and Tiantao Cheng[2]

1. Environmental Research Center, Duke Kunshan University, Kunshan 215316, China

2. Department of Atmospheric and Oceanic Sciences & Institute of Atmospheric Sciences, Fudan University, Shanghai 200438, China

Corresponding author: Weijie Wang (wang.weijie@dukekunshan.edu.cn)

Key Points:

- Dust emission in East Asia will decrease during the twenty-first century due to the reduction of surface winds under the warming climate
- The percentage of dust emission reduction depends on the magnitude of warming
- In the extreme warming scenario, dust optical depth over source regions in East Asia will decrease by 5.6% by the end of the 21st century

Abstract

A reduction of dust emission over the major dust source regions in East Asia in the twenty-first century is diagnosed in the climate change simulations of the Sixth Climate Model Intercomparison Project (CMIP6). Such change is attributable to the reduction of surface wind speeds in the dust source regions. To evaluate how the magnitude of warming affects dust emission, we examined two model scenarios, one high-forcing pathway and one medium-forcing pathway. We find dust optical depth over dust source regions would decrease by 5.6% by the end of the twenty-first century under the high-forcing pathway. Under the medium-forcing pathway, dust optical depth would decrease by less than 2%. These results provide a quantitative understanding of how global warming affects dust emission in the major dust source regions in East Asia.

Plain Language Summary

Over the past half-century, dust emission in the major dust source regions in East Asia exhibited a downward trend due to reduced surface winds. It has been pointed out that such a trend will continue in the twenty-first century under global warming. However, the magnitude of the reduction is unclear. Here we attempt to evaluate quantitatively how dust emission in East Asia will vary in the twenty-first century under two warming scenarios using climate models. We find dust optical depth, which is closely associated with dust emission, will decrease by 5.6% under the extreme warming scenario, while it will decrease by less than 2% in the medium warming scenario. Thus, we suggest that the variability of dust, which is not included in most climate models, needs to be taken into consideration for understanding the dust-climate feedback.

1 Introduction

Dust emission in East Asia is estimated to account for 11% of the global dust emission (Kok et al., 2021). Dust originated in East Asia can transport downwind by westerlies across the Pacific to North America (Hu et al., 2019; Voss et al., 2020), affecting air quality (Wang et al., 2010), radiative balance (Stanelle et al., 2014), and ocean biogeochemistry along the way (Jickells et al., 2005).

Dust emission in East Asia undergoes interannual variability and is known to be associated with a number of factors, such as surface wind speeds, precipitation, and surface temperatures in the source regions (Guan et al., 2017; Kurosaki & Mikami, 2003; Wu et al., 2021). It is also known that dust emission in East Asia is associated with atmospheric circulations (Zhu et al., 2008) and oceanic oscillations such as the Pacific decadal oscillation (Gong et al., 2006). Dust events frequency in East Asia has exhibited a downward trend since the 1950s (Tan et al., 2014; Wu et al., 2021; Zhao et al., 2004), and such trend is attributed to reduced wind speeds (Guan et al., 2017; Wu et al., 2021; Xu et al., 2020), enhanced precipitation (Wang, 2005), and increasing surface temperatures (Guan et al., 2017; Wu et al., 2021). Among these factors that affect dust emission, winds are found to play a dominant role (Gong et al., 2006; Guo et al., 2019).

Although it has been found that dust emission in the major dust source regions would decrease in East Asia under the warming climate during the twenty-first century (Liu et al., 2020; Zong et al., 2021), the magnitude of reduction remains unclear and warrants further investigation. In this work, we propose using surface wind speeds alone to estimate dust emission in East Asia during the twenty-first century using two scenarios of the Sixth Climate Model Intercomparison Project (CMIP6), namely, one high-forcing pathway and one medium-forcing pathway. Both scenarios show a statistically significant downward trend in dust emission over the major dust source regions in East Asia during the twenty-first century under a warming climate.

2 Data

Here we use the Deep Blue and Dark Target combined aerosol optical depth from the level 3 daily aerosol products from the Moderate Resolution Imaging Spectroradiometer (MODIS) Aqua platform (Platnick et al., 2017) to study dust optical depth (DOD) over the major dust source regions in China from 2003 through 2020. In order to eliminate other types of aerosols to obtain DOD, the following three criteria were applied based on previous works. First, the Angstrom exponent is less than 0.6 (Schepanski et al., 2007). Since dust is mostly coarse particles, this criterion excludes fine aerosols (Dubovik et al., 2002). Second, the single scattering albedo (SSA) is less than 0.95. This criterion effectively excludes sea salt in the coastal regions as sea salt has an SSA close to 1 (Ginoux et al., 2012). Third, the SSA at 412 nm is less than that at 670 nm as dust absorption increases from red to blue. Daily mean DOD from MODIS is used to construct monthly mean and long-term mean DOD. The spatial resolution of DOD is at 1° longitude by 1° latitude.

To understand the effect of surface winds on DOD, we use monthly mean wind speeds at 10 m above the surface to construct the relationship between surface winds and DOD. Monthly mean wind speeds at 10 m were taken from the European Centre for Medium-Range Weather Forecasts Reanalysis v5 (ERA5) from 2003 through 2020 (Muñoz Sabater, 2019). We also use monthly mean precipitation from the Global Precipitation Climatology Project (GPCP) Version 2 (Adler et al., 2003) to construct the climatology of precipitation from 1979 through 2020 in the major dust source regions.

Monthly mean wind speeds at 10 m from two scenarios of CMIP6 were selected to estimate the future change of dust. The two scenarios used in this work are the shared socioeconomic pathway 2 with radiative forcing reaching a level of 4.5 Wm^{-2} in 2100 (ssp245), a medium-forcing pathway, and the shared socioeconomic pathway 5 with radiative forcing reaching a level of 8.5 Wm^{-2} in 2100 (ssp585), a high-forcing pathway. Only models with both scenarios were selected in this work, and all ensemble members of each model were included for estimating the future change of dust in East Asia. Table 1 summarizes the modeling centers, model names, and ensemble members for both scenarios used in this work.

Table 1. CMIP6 models used in this work. Shown are the modeling centers, model names, and ensemble members for both scenarios.

Institution	Model	ssp245	ssp585
Commonwealth Scientific and Industrial Research Organisation and Bureau of Meteorology (CSRIO; Australia)	ACCESS-CM2	5	5
	ACCESS-ESM1-5	40	10
Alfred Wegener Institute (AWI; Germany)	AWI-CM-1-1-MR	1	1
Chinese Academy of Meteorological Sciences (CAMS; China)	CAMS-CSM1-0	2	2
Chinese Academy of Sciences (CAS; China)	CAS-ESM2-0	2	2
National Center for Atmospheric Research (NCAR; United States)	CESM2	3	3
	CESM2-WACCM	5	5
Centro Euro-Mediterraneo sui Cambiamenti Climatici (CMCC; Italy)	CMCC-CM2-SR5	1	1
	CMCC-CM2-ESM2	1	1
Centre National de Recherches Météorologique (CNRM; France)	CNRM-CM6-1	6	6
	CNRM-CM6-1-HR	1	1
	CNRM-ESM2-1	10	5
Canadian Centre for Climate Modeling and Analysis (CCCma; Canada)	CanESM5	50	50
European consortium (EC)	EC-Earth3	1	1
	EC-Earth3-CC	1	1
Chinese Academy of Sciences (CAS; China)	FGOALS-f3-L	1	1
First Institute of Oceanography, Ministry of Natural Resources (FIO; China)	FIO-ESM2.0	3	3
National Oceanic and Atmospheric Administration Geophysical Fluid Dynamic Laboratory (GFDL; United States)	GFDL-ESM4	1	1
National Aeronautics and Space Administration Goddard Institute for Space Studies (GISS; United States)	GISS-E2-1-G	30	11
Met Office Hadley Centre (MOHC; United Kingdom)	HadGEM3-GC31-LL	5	4
Indian Institute of Tropical Meteorology (IITM; India)	IITM-ESM	1	1
Institute for Numerical Mathematics (INM; Russia)	INM-CM4-8	1	1
	INM-CM5-0	1	1

Institut Pierre-Simon Laplace (IPSL; France)	IPSL-CM6A-LR	11	6
National Institute of Meteorological Science-Korea Meteorological Administration (NIMS-KMA; Korea)	KACE1-0-G	3	3
Korea Institute of Ocean Science and Technology (KIOST; Korea)	KIOST-ESM	1	1
Model for Interdisciplinary Research on Climate (MIROC; Japan)	MIROC-ES2L	30	11
	MIROC6	33	50
Max Planck Institute for Meteorology (MPI; Germany)	MPI-ESM1-2-HR	2	2
	MPI-ESM1-2-LR	30	10
Meteorological Research Institute (MRI; Japan)	MRI-ESM2-0	5	6
Nanjing University of Information Science and Technology (NUIST; China)	NESM3	2	2
Norwegian Climate Centre (NCC; Norway)	NorESM2-LM	13	1
	NorESM2-MM	1	1
National Center for Atmospheric Research (NCAR; Taiwan, China)	TaiESM1	1	1
Met Office Hadley Centre (MOHC; United Kingdom)	UKESM1.0-LL	6	5

3 Results

3.1 DOD and 10 m wind speeds

The two major dust source regions in East Asia include the Taklamakan Desert in northwestern China and the Gobi Desert in Northern China (Figure 1a). The long-term mean DOD from satellite from 2003 through 2020 over the major dust source regions is 0.15 (Figure 1a). The Taklamakan Desert is an extreme arid region with a mean annual precipitation of 100 mm, while the Gobi Desert is an arid region with a mean annual precipitation of 223 mm averaged from 1979 through 2020 using GPCP (Figure 1a). Although it has been observed that the annual precipitation over these major dust source regions has been increasing over the past half-century (Su et al., 2020) and the increase in precipitation can strengthen soil cohesion and enhance vegetation cover, thus reducing dust emission, previous studies found no correlation between vegetation and dust emission in northwestern China as vegetation there is sparse (Zhang et al., 2003; Zou & Zhai, 2004). In addition, the correlation between soil moisture and dust emission is much weaker compared with that between surface wind speeds and dust emission in this region (Guo et al., 2019; Wu et al., 2021).

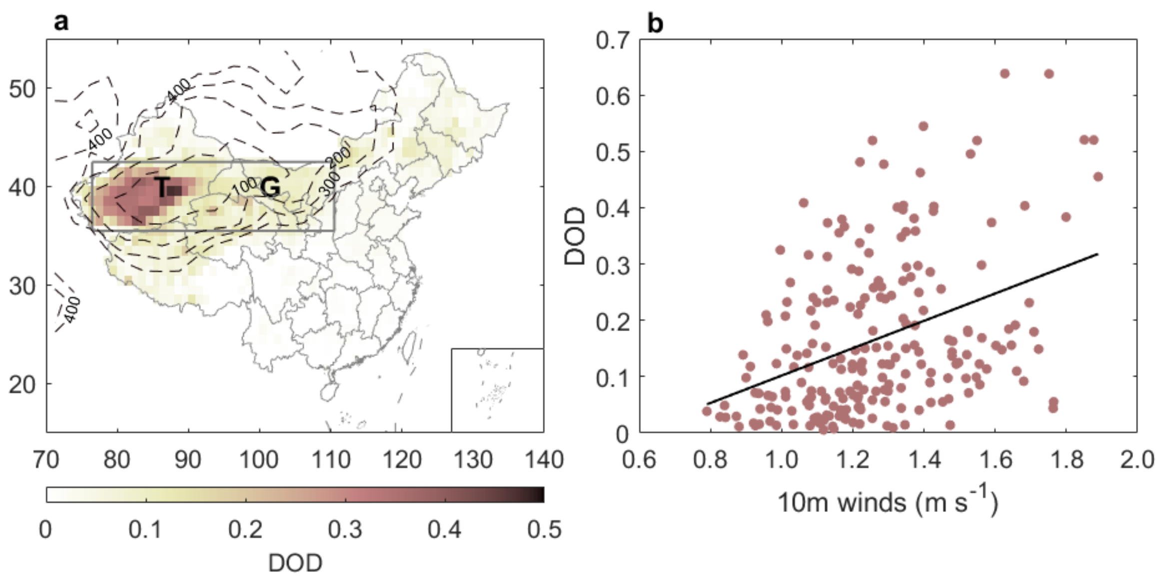

Figure 1. Long-term mean DOD and precipitation and the relationship between DOD and 10 m winds. (a) Long-term mean DOD at 1° by 1° over China from 2003 through 2020 using MODIS daily DOD. The contour lines are the mean annual precipitation in mm using monthly mean precipitation from GPCP from 1979 through 2020. The gray box indicates the major dust source regions (74.5° to 110.5°E, 35.5° to 42.5°N). T and G indicate locations of the Taklamakan Desert and the Gobi Desert, respectively. (b) Scatterplot of monthly mean DOD as a function of monthly mean 10 m winds averaged over the major dust source regions from 2003 through 2020. Monthly mean 10 m winds are from ERA5. The black line is the least-squares regression line described by the equation $y = 0.24x – 0.14$.

The relationship between dust emission and surface wind speeds is well-established (Fécan et al., 1999). The monthly mean DOD averaged over the major dust source regions exhibits a statistically significant correlation with the monthly mean 10 m wind speeds averaged over the same region from 2003 through 2020 (Figure 1b). The correlation between 10 m wind speeds from ERA5 and DOD from MODIS is 0.4 ($p < 0.01$), indicating that 10 m wind speeds can be used to approximate DOD at the monthly scale, which is closely associated with dust emission in the source regions. Such correlation between satellite-retrieved DOD and wind speeds from other reanalyses, such as the Modern-Era Retrospective analysis for Research and Application, Version 2, is also robust. Since surface winds from ERA5 offer the best agreement among reanalyses when compared with in situ observations (Ramon et al., 2019), in this work, the relationship between DOD and 10 m wind speeds from ERA5 is used to estimate DOD over the major dust source regions in East Asia during the twenty-first century.

3.2 DOD during the twenty-first century

Figure 2 shows the estimates of DOD over the major dust source regions in East Asia during the twenty-first century using 10 m winds from two scenarios of CMIP6. As winds from models vary significantly due to the model's internal variability, wind speeds from each model are scaled so that the mean wind speeds from each model are equal to those from ERA5 for the period of 2015 through 2020. In the ssp585 scenario, the multimodel mean time series shows a statistically significant downward trend of -0.008 ± 0.0003 in DOD per 100 years (Figure 2a), representing roughly a $5.6\pm0.2\%$ reduction of the long-term mean DOD obtained from MODIS for the period from 2003 through 2020.

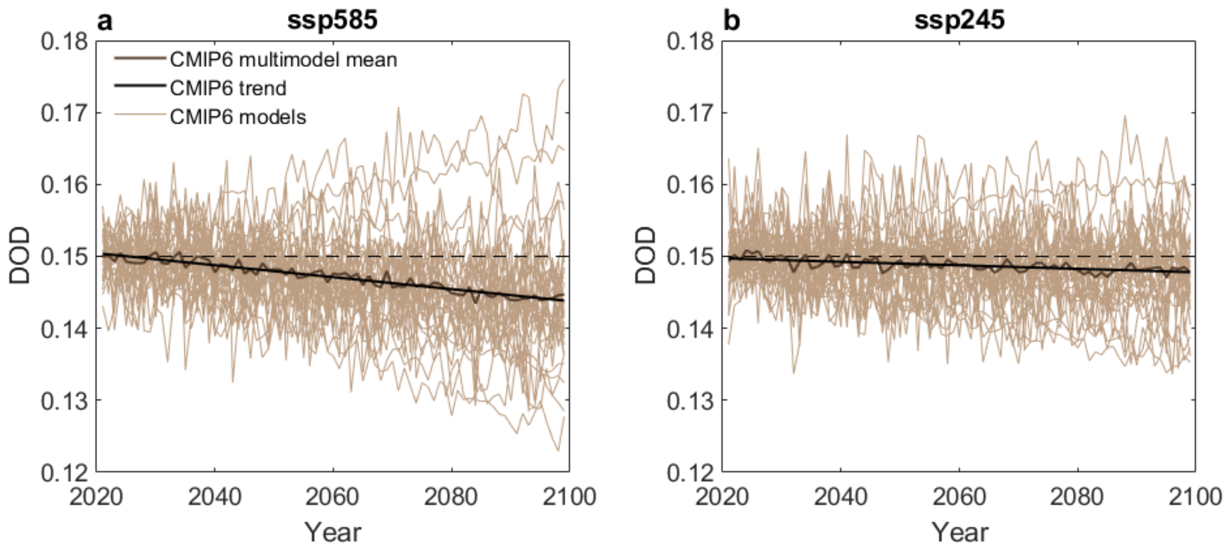

Figure 2. Time series of DOD over the major dust source regions during the twenty-first century. (a) The CMIP6 ensemble mean time series, the multimodel mean time series and its linear trend estimated using monthly mean 10 m winds from ssp585 of CMIP6. (b) The same as (a) using monthly 10 m winds from ssp245.

Among the 36 models considered here, 30 models exhibit statistically significant downward trends in DOD, while only four models exhibit statistically significant upward trends in DOD (Figure 3a). The same analysis was repeated using the ssp245 scenario, in which the multimodel mean time series shows a statistically significant downward trend of -0.0024±0.0003 in DOD per 100 years, 30% of that for the ssp585 scenario (Figure 2b). 16 of the 36 models exhibit statistically significant downward trends in DOD, while four models exhibit statistically significant upward trends in DOD (Figure 3b).

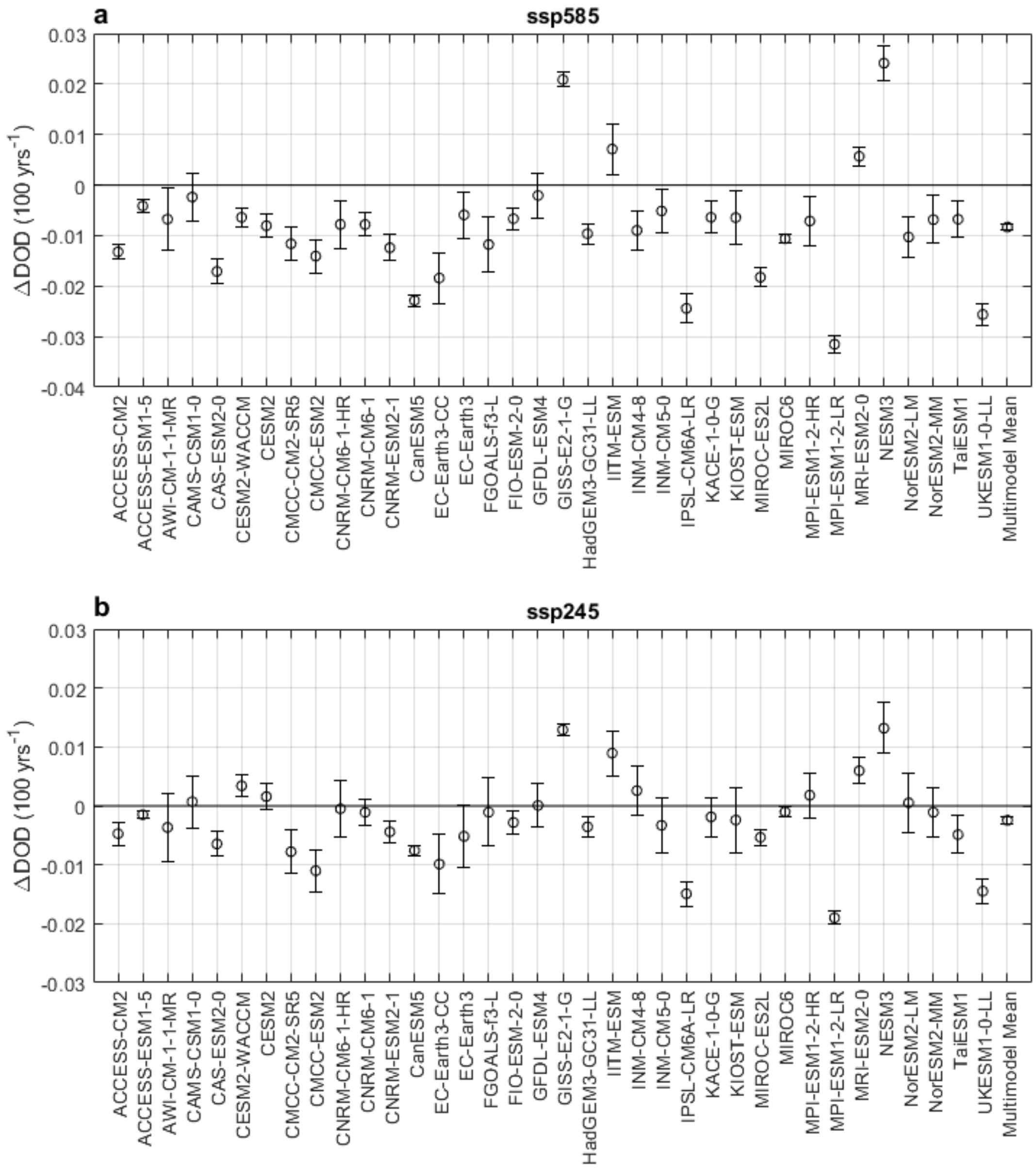

Figure 3. CMIP6 ssp585 and ssp245 twenty-first century trends in DOD. (a) The linear trend and 95% confidence intervals of the ensemble mean and the multimodel mean trend for ssp585. (b) The same as (a) but for ssp245.

4 Discussion

This decline in DOD indicates that dust emission in the major dust source regions in East Asia will decrease during the twenty-first century, which would likely contribute to the improvement of air quality in the dust source regions and downwind regions, especially in the springtime, when dust events are frequent. Under the warming climate, not only dust emission in East Asia will decline, but in other major dust source regions, such as the Saharan Desert, the largest desert in the world, dust emission will also decline due to reduced surface wind speeds (Evan et al., 2016). In addition, decreasing dust has been observed in the Middle East over the past decade as a result of enhanced soil moisture and precipitation and reduced surface wind speeds (Xia et al., 2022).

So far, the radiative effect dust has on climate is uncertain. It is known that dust reflects shortwave radiation, but how dust interacts with longwave radiation is less clear. As large particles can absorb longwave radiation more effectively, the radiative effect of dust depends on the size of the particle (Mahowald et al., 2014). On the global scale, the direct radiative effect of dust is estimated to be between -0.48 and +0.2 Wm^{-2} (Kok et al., 2017). But on the regional scale, the direct radiative effect of dust can be one order of magnitude larger. For example, during a two-week observation in Zhangye, located between the Taklamakan and Gobi Deserts, the direct longwave radiative effect of dust was estimated to vary between 2.3 and 20 Wm^{-2}, compensating for over one-half of the shortwave cooling effect at the surface (Hansell et al., 2012). Given the radiative effect of dust, the decrease in dust emission in the twenty-first century will inevitably affect the energy balance of the surface and the atmosphere, particularly in the source regions.

Currently, the interannual variability of dust is not included in most climate models. In addition, the indirect effects of dust on climate are poorly understood. Thus, efforts should be given to better represent dust variability in models to understand and predict the dust-climate feedback in the future.

5 Conclusions

This work estimated the trend of East Asia dust during the twenty-first century under two warming scenarios. We did so by examining DOD, derived from surface winds in CMIP6 models, over the major dust source regions. Under the high-forcing pathway, that is, radiative forcing reaching a level of 8.5 Wm^{-2} in 2100, DOD in East Asia is estimated to reduce by 5.6% compared with the mean DOD from 2003 through 2020 over the dust source regions. Under the medium-forcing pathway, that is, radiative forcing reaching a level of 4.5 Wm^{-2} in 2100, DOD in East Asia is estimated to reduce by less than 2%. It is worth noting that such estimations did not take into consideration the complex dust-climate feedback that is not well understood, nor did they include other factors that may affect dust emission, such as land use change. Nevertheless, our results provide a quantitative understanding of East Asia dust emission in the twenty-first century and indicate that the degree dust emission responds to climate change varies with the magnitude of warming.

Acknowledgments

This work is supported by the National Natural Science Foundation of China (Grant No. 42175179) and the Natural Science Foundation of Shanghai (Grant No. 22ZR1404000). The authors acknowledge the World Climate Research Program's Working Group for making available the CMIP6 output.

Conflict of Interest

The authors declared no conflict of interest relevant to this study.

Open Research

MODIS Aqua level 3 daily aerosol products are ordered from https://dx.doi.org/10.5067/MODIS/MYD08_D3.061. ERA5 monthly mean 10 m winds are available at https://doi.org/10.24381/cds.68d2bb30. GPCP data are available at https://psl.noaa.gov/data/gridded/data.gpcp.html. CMIP6 data are available through the Earth System Grid Federation at https://pcmdi.llnl.gov/CMIP6/. The CMIP6 models in this work are listed in Table 1.

References

Adler, R. F. Huffman, G. J., Chang, A., Ferraro, R., Xie, P.-P., Janowiak, J., Rudolf, B., Scheneider, Udo, Curtis, S., Bolvin, D., Gruber, A., Susskind, J., Arkin, P., & Nelkin, E. (2003). The version 2 Global Precipitation Climatology Project (GPCP) monthly precipitation analysis (1979-present). *Journal of Hydrometeorology*, *4*(6), 1147-1167. https://doi.org/10.1175/1525-7541(2003)004<1147:TVGPCP>2.0.CO;2

Dubovik, O., Holben, B., Eck, T. F., Smirnov, A., Kaufman, Y. J., King, M. D., Tanré, D., & Slutsker, I. (2002). Variability of absorption and optical properties of key aerosol types observed in worldwide locations. *Journal of the Atmospheric Sciences*, *59*, 590–608.

Evan, A. T., Flamant, C., Gaetani, M., & Guichard, F. (2016). The past, present and future of African dust. *Nature*, *531*(7595), 493–495. https://doi.org/10.1038/nature17149

Fécan, F., Marticorena, B., & Bergametti, G. (1999). Parametrization of the increase of the aeolian erosion threshold wind friction velocity due to soil moisture for arid and semi-arid areas. *Annales Geophysicae*, *17*, 149–157.

Ginoux, P., Prospero, J. M., Gill, T. E., Hsu, N. C., & Zhao, M. (2012). Global-scale attribution of anthropogenic and natural dust sources and their emission rates based on MODIS Deep Blue aerosol products. *Reviews of Geophysics*, *50*(3). https://doi.org/10.1029/2012RG000388

Gong, S. L., Zhang, X. Y., Zhao, T. L., Zhang, X. B., Barrie, L. A., Mckendry, I. G., & Zhao, C. S. (2006). A simulated climatology of Asian dust aerosol and its trans-pacific transport. Part II: Interannual variability and climate connections. *Journal of Climate*, *19*(1), 104–122. https://doi.org/10.1175/JCLI3606.1

Guan, Q., Sun, X., Yang, J., Pan, B., Zhao, S., & Wang, L. (2017). Dust storms in northern China: Long-term spatiotemporal characteristics and climate controls. *Journal of Climate*, *30*(17), 6683–6700. https://doi.org/10.1175/JCLI-D-16-0795.1

Guo, J., Xu, H., Liu, L., Chen, D., Peng, Y., Yim, S. H. L., Yang, Y., Li, J., Zhao, C., & Zhai, P. (2019). The Trend Reversal of Dust Aerosol Over East Asia and the North Pacific Ocean Attributed to Large-Scale Meteorology, Deposition, and Soil Moisture. *Journal of Geophysical Research: Atmospheres*, *124*(19), 10450–10466. https://doi.org/10.1029/2019JD030654

Hansell, R. A., Tsay, S. C., Hsu, N. C., Ji, Q., Bell, S. W., Holben, B. N., Welton, E. J., Roush, T. L., Zhang, W., Huang, J., Li, Z., & Chen, H. (2012). An assessment of the surface longwave direct radiative effect of airborne dust in Zhangye, China, during the Asian Monsoon Years field experiment (2008). *Journal of Geophysical Research Atmospheres*, *117*(13). https://doi.org/10.1029/2011JD017370

Hu, Z., Huang, J., Zhao, C., Bi, J., Jin, Q., Qian, Y., Leung, L. R., Feng, T., Chen, S., & Ma, J. (2019). Modeling the contributions of Northern Hemisphere dust sources to dust outflow from East Asia. *Atmospheric Environment*, *202*, 234–243. https://doi.org/10.1016/j.atmosenv.2019.01.022

Jickells, T. D., An, Z. S., Andersen, K. K., Baker, A. R., Bergametti, G., Brooks, N., Cao, J. J., Boyd, P. W., Duce, R. A., Hunter, K. A., Kawahata, H., Kubilay, N., laRoche, J., Liss, P. S., Mahowald, N., Prospero, J. M., Ridgwell, A. J., Tegen, I., & Torres, R. (2005). Global iron connections between desert dust ocean biogeochemistry and climate. *Science*, *308*(5718), 67–71.

Kok, J. F., Adebiyi, A. A., Albani, S., Balkanski, Y., Checa-Garcia, R., Chin, M., Colarco, P. R., Hamilton, D. S., Huang, Y., Ito, A., Klose, M., Li, L., Mahowald, N. M., Miller, R. L., Obiso, V., Pérez García-Pando, C., Rocha-Lima, A., & Wan, J. S. (2021). Contribution of the world's main dust source regions to the global cycle of desert dust. *Atmospheric Chemistry and Physics*, *21*(10), 8169–8193. https://doi.org/10.5194/acp-21-8169-2021

Kok, J. F., Ridley, D. A., Zhou, Q., Miller, R. L., Zhao, C., Heald, C. L., Ward, D. S., Albani, S., & Haustein, K. (2017). Smaller desert dust cooling effect estimated from analysis of dust size and abundance. *Nature Geoscience*, *10*(4), 274–278. https://doi.org/10.1038/ngeo2912

Kurosaki, Y., & Mikami, M. (2003). Recent frequent dust events and their relation to surface wind in East Asia. *Geophysical Research Letters*, *30*(14). https://doi.org/10.1029/2003GL017261

Liu, J., Wu, D., Liu, G., Mao, R., Chen, S., Ji, M., Fu, P., Sun, Y., Pan, X., Jin, H., Zhou, Y., & Wang, X. (2020). Impact of Arctic amplification on declining spring dust events in East Asia. *Climate Dynamics*, *54*(3–4), 1913–1935. https://doi.org/10.1007/s00382-019-05094-4

Mahowald, N., Albani, S., Kok, J. F., Engelstaeder, S., Scanza, R., Ward, D. S., & Flanner, M. G. (2014). The size distribution of desert dust aerosols and its impact on the Earth system. *Aeolian Research, 15*, 53–71. https://doi.org/10.1016/j.aeolia.2013.09.002

Muñoz Sabater, J. (2019). ERA5-Land monthly averaged data from 1981 to present. Copernicus Climate Change Service (C3S) Climate Data Store (CDS). (Accessed on < 27-10-2021 >). 10.24381/cds.68d2bb3

Platnick, S., King, M., & Hubanks, P. (2017). MODIS Atmosphere L3 Daily Product. NASA MODIS Adaptive Processing System, Goddard Space Flight Center. https://dx.doi.org/10.5067/MODIS/MYD08_D3.061

Ramon, J., Lledó, L., Torralba, V., Soret, A., & Doblas-Reyes, F. J. (2019). What global reanalysis best represents near-surface winds? *Quarterly Journal of the Royal Meteorological Society*, *145*(724), 3236–3251. https://doi.org/10.1002/qj.3616

Schepanski, K., Tegen, I., Laurent, B., Heinold, B., & Macke, A. (2007). A new Saharan dust source activation frequency map derived from MSG-SEVIRI IR-channels. *Geophysical Research Letters*, *34*(18). https://doi.org/10.1029/2007GL030168

Stanelle, T., Bey, I., Raddatz, T., Reick, C., & Tegen, I. (2014). Anthropogenically induced changes in twentieth century mineral dust burden and the associated impact on radiative forcing. *Journal of Geophysical Research*, *119*(23), 13,526-13,546. https://doi.org/10.1002/2014JD022062

Su, Y., Zhao, C., Wang, Y., & Ma, Z. (2020). Spatiotemporal variations of precipitation in China using surface gauge observations from 1961 to 2016. *Atmosphere*, *11*(3), 303. https://doi.org/10.3390/atmos11030303

Tan, M., Li, X., & Xin, L. (2014). Intensity of dust storms in China from 1980 to 2007: A new definition. *Atmospheric Environment*, *85*, 215–222. https://doi.org/10.1016/j.atmosenv.2013.12.010

Voss, K. K., Evan, A. T., Prather, K. A., & Ralph, A. F. M. (2020). Dusty Atmospheric Rivers: Characteristics and Origins. *Journal of Climate*, *33*, 9749–9762. https://doi.org/10.1175/JCLI-D-20

Wang, N. (2005). Decrease trend of dust event frequency over the past 200 years recorded in the Malan ice core from the northern Tibetan Plateau. *Chinese Science Bulletin*, *50*(24), 2866–2871. https://doi.org/10.1360/982005-237

Wang, W., Cheng, T., Zhang, R., Jia, X., Han, Z., Zhang, X., Xu, X., & Li, D. (2010). Insights into an Asian dust event sweeping Beijing during April 2006: Particle chemical composition, boundary layer structure, and radiative forcing. *Journal of Geophysical Research Atmospheres*, *115*(18). https://doi.org/10.1029/2009JD013391

Wu, D., Liu, J., Wang, T., Niu, X., Chen, Z., Wang, D., Zhang, X., Ji, M., Wang, X., & Pu, W. (2021). Applying a dust index over North China and evaluating the contribution of potential factors to its distribution. *Atmospheric Research*, *254*. https://doi.org/10.1016/j.atmosres.2021.105515

Xia, W., Wang, Y., & Wang, B. (2022). Decreasing Dust Over the Middle East Partly Caused by Irrigation Expansion. *Earth's Future*, *10*(1). https://doi.org/10.1029/2021EF002252

Xu, C., Guan, Q., Lin, J., Luo, H., Yang, L., Tan, Z., Wang, Q., Wang, N., & Tian, J. (2020). Spatiotemporal variations and driving factors of dust storm events in northern China based on high-temporal-resolution analysis of meteorological data (1960–2007). *Environmental Pollution*, *260*. https://doi.org/10.1016/j.envpol.2020.114084

Zhang, X. Y., Gong, S. L., Zhao, T. L., Arimoto, R., Wang, Y. Q., & Zhou, Z. J. (2003). Sources of Asian dust and role of climate change versus desertification in Asian dust emission. *Geophysical Research Letters*, *30*(24). https://doi.org/10.1029/2003GL018206

Zhao, C., Dabu, X., & Li, Y. (2004). Relationship between climatic factors and dust storm frequency in Inner Mongolia of China. *Geophysical Research Letters*, *31*(1). https://doi.org/10.1029/2003GL018351

Zhu, C., Wang, B., & Qian, W. (2008). Why do dust storms decrease in northern China concurrently with the recent global warming? *Geophysical Research Letters*, *35*(18). https://doi.org/10.1029/2008GL034886

Zou, X. K., & Zhai, P. M. (2004). Relationship between vegetation coverage and spring dust storms over northern China. *Journal of Geophysical Research: Atmospheres*, *109*(3). https://doi.org/10.1029/2003jd003913